第 28 卷 第 5 期　　焊 接 学 报　　Vol. 28 No. 5
2007 年 5 月　　TRANSACTIONS OF THE CHINA WELDING INSTITUTION　　May 2007

镁合金激光氩弧复合热源冷填丝焊接工艺

郝新锋，　刘黎明，　李长茂
（大连理工大学 三束材料改性国家重点实验室，辽宁 大连　116024）


郝新锋

摘　要：研究了镁合金的低功率激光—氩弧复合热源冷填丝焊接工艺。通过5 mm厚镁合金板材的堆焊试验，研究了焊接电流、焊接速度、钨极高度和热源距离等参数对焊缝成形和焊接熔深的影响，确定了钨极高度为0.75 mm，热源间距 D_{LA} 为1.2 mm左右的焊接参数范围；在堆焊基础上，进行了2.5 mm厚镁合金板材的对焊试验，实现了单面焊双面成形，焊接速度达1 200 mm/min，焊接接头熔深为单TIG 冷填丝接头熔深的两倍，抗拉强度达到母材的95%左右，实现了高速、优质的镁合金冷填丝焊接。另外，简要分析了激光的加入对焊接过程的影响。

关键词：镁合金；低功率激光；复合热源；冷填丝焊接
中图分类号：TG406　　文献标识码：A　　文章编号：0253—360X(2007)05—077—04

0　序　　言

镁合金具有比重轻、比强度和比刚度高、易于机械加工等优点[1]，在航空航天、汽车等行业具有广阔的应用前景。工业生产中多采用手工填丝的方法焊接镁合金结构件，该方法焊接速度慢，仅适于小批量生产，并且焊接质量主要依靠工作者的经验与熟练程度，具有极大的不稳定性[2]。所以开发高效优质的镁合金填丝焊接工艺，尤其是提高填丝焊接的自动化程度和焊接质量是目前亟待解决的问题。

镁合金填丝焊接包括冷填丝焊接和 MIG 焊接两种方法。目前MIG 焊接方面，德国Wohlfahrt，Helmut 等人通过修改焊接电流波形，改变热输入实现了镁合金的 MIG 焊接，但疲劳强度仅为母材的50%，消除余高强化后也仅为母材的 75%[3]。冷填丝焊接方面，大连理工大学董长富等人研究了单TIG冷填丝焊接，焊接接头的抗拉强度达到母材的 94%，但是焊接速度只有 600～800 mm/min，无法实现高速焊接[4]。

利用低功率激光—氩弧复合热源冷填丝焊接的方法对5 mm厚镁合金板材进行堆焊试验，研究了焊接电流、焊接速度等焊接参数对焊缝成形的影响。在此基础上进行2.5 mm厚镁合金板材的对焊试验，实现了单面焊双面成形，并对焊接接头进行了拉伸性能测试。

1　试　　验

1.1　试验材料

试验材料为2.5，5 mm厚的镁合金 AZ31B 板材，尺寸为300 mm×120 mm；焊丝采用自制的 ϕ1.2 mm 镁合金焊丝。母材和焊丝的化学成分如表 1 所示。焊接前镁合金板、焊丝须经砂纸打磨，然后用丙酮清洗去除表面的油脂和氧化膜。

表 1　母材及焊丝的化学成分(质量分数，%)
Table 1　Chemical composition of base metal and welding wire

	Al	Zn	Mn	Ca	Si	Cu	Ni	Fe	Mg
母材	3.27	0.92	0.25	＜0.04	＜0.10	＜0.05	＜0.005	＜0.005	余量
焊丝	6.29	0.95	0.25	＜0.04	＜0.10	＜0.05	＜0.005	＜0.005	余量

1.2　试验方法

试验采用低功率激光—氩弧复合热源冷填丝焊接的方法焊接镁合金板材，试验原理如图 1 所示。其中热源间距 D_{LA} 表示激光作用点与钨极端点之间的距离，脉冲 YAG 激光频率为39 Hz，输出功率为300 W，离焦量为－1 mm，焊丝与母材的夹角和焊枪

收稿日期：2006—06—19
基金项目：大连理工大学—沈阳自动化研究所联合探索基金

角度 α 均为 45°，在整个焊接过程中保持不变。焊接时电弧在前激光在后。

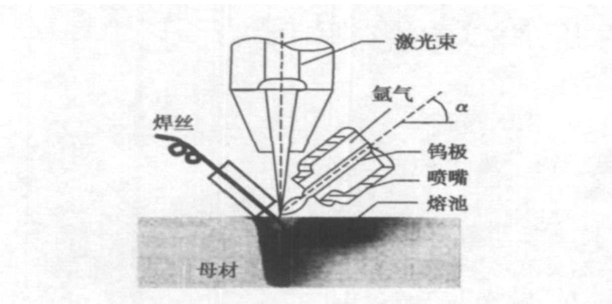

图 1 激光—氩弧复合热源冷填丝焊接原理图

Fig. 1 Schematic diagram laser-arc hybrid welding with filler metal

2 试验结果及分析

2.1 镁合金堆焊试验

对5 mm厚的AZ31板材进行复合热源冷填丝堆焊试验，研究焊接参数对焊缝熔深、熔宽及余高的影响，确定复合热源冷填丝焊接工艺的参数范围。

2.1.1 焊接电流对焊缝成形的影响

图2 表示焊接速度为800 mm/min，送丝速度为2.5 m/min，钨极高度为0.75 mm，热源间距为1.2 mm时，焊接电流对焊缝成形的影响。

当电流较小时，焊缝熔深和熔宽都比较小，这是因为电弧对母材和焊丝的热输入小，熔化效率低，焊丝不能及时熔化，当未熔焊丝伸至激光作用点和电弧中心时，会阻碍激光和电弧对母材的加热，大大减弱母材的熔化效率；同时焊丝在激光和电弧中心弧柱的作用下会被急剧加热而熔化，所以焊接过程中多以较大的熔滴形式向熔池过渡，造成焊丝的熔敷时断时续，焊接过程不稳定，从而造成焊缝表面的局部塌陷和凸起现象，成形比较差。当电流增大时，电弧能量增强，焊缝熔深和熔宽都相应增大；同时大的热输入使焊丝熔化充分、均匀，熔敷效果得到改善，焊缝成形美观，呈波纹状。由于送丝速度保持不变，单位时间内的熔敷量一定，所以随着焊缝熔深和熔宽的增大，焊缝余高逐渐减小。试验中送丝速度选取2.5 m/min，为了保证熔深和余高的合理分配，电流应控制在130～140 A。

2.1.2 焊接速度对焊缝成形的影响

由图 3 可以看出在其它参数相同的情况下（焊接电流为140 A，送丝速度为2.5 m/min，钨极高度为0.75 mm，热源间距为1.2 mm），随着焊接速度的增大，焊缝熔深、熔宽和余高都相应地减小。这是因为在焊接过程中，单位时间内对母材的热输入与焊接速度成反比，焊接热输入的减小降低了对母材和焊丝的熔化效率，而且镁合金导热速度快，从而造成熔

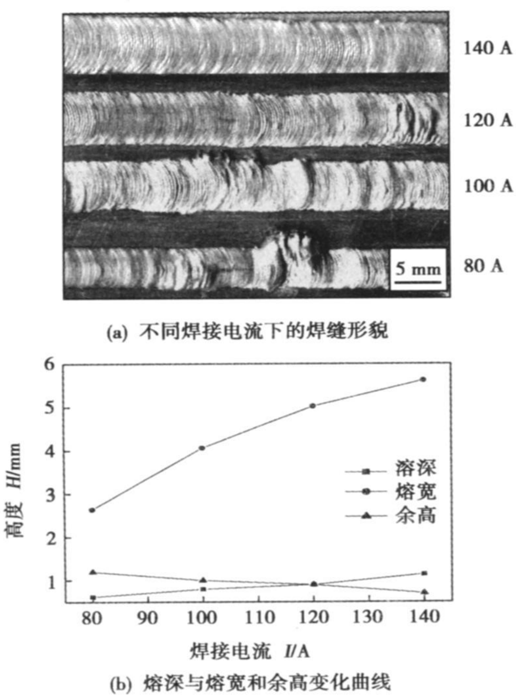

图 2 焊接电流对焊缝成形的影响

Fig. 2 Effect of welding current on weld appearance

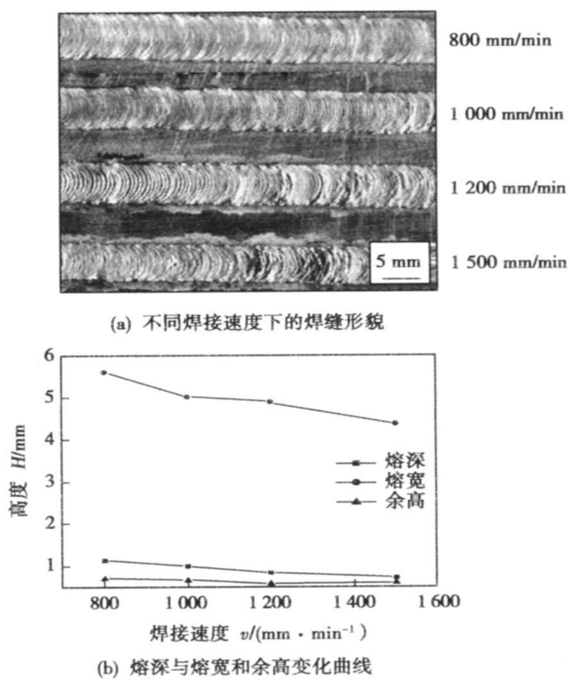

图 3 焊接速度对焊缝成形的影响

Fig. 3 Effect of welding speed on weld appearance

深和熔宽急剧减小。同时焊接速度越高电弧稳定性越差, 造成焊丝熔化不连续, 因而造成焊缝成形不规则。由图 3 可知, 随着焊接速度的增大, 焊缝由连续致密的波纹状变得断断续续, 凸凹不平。试验中焊接速度取1 000~1 200 mm/min。

2.1.3　钨极高度对焊缝成形的影响

图4 为其它参数相同(焊接电流为140 A, 焊接速度为800 mm/min, 热源间距为1.2 mm, 送丝速度为2.5 m/min), 改变钨极高度时焊缝成形的变化情况。随着钨极高度的增大, 熔深和熔宽都是先增大后减小。当钨极高度为0.5 mm时, 焊缝成形好, 条纹致密, 但熔深和熔宽较小。当钨极高度增大到0.75 mm时, 电弧对熔池的冲击作用增强, 从而增大了焊缝熔深。钨极高度增大到1.0 mm时, 电弧电压增大, 电弧加热功率加大, 但是电弧热源半径增大, 对母材的热输入减小, 熔深略有减小而熔宽增大。当钨极高度继续增大时, 热输入进一步减小, 造成焊缝熔深和熔宽都减小; 同时电弧稳定性下降, 造成焊缝表面成形比较差。为了保证焊接过程的稳定性及焊缝的良好成形, 试验中钨极高度一般取0.75 mm左右。

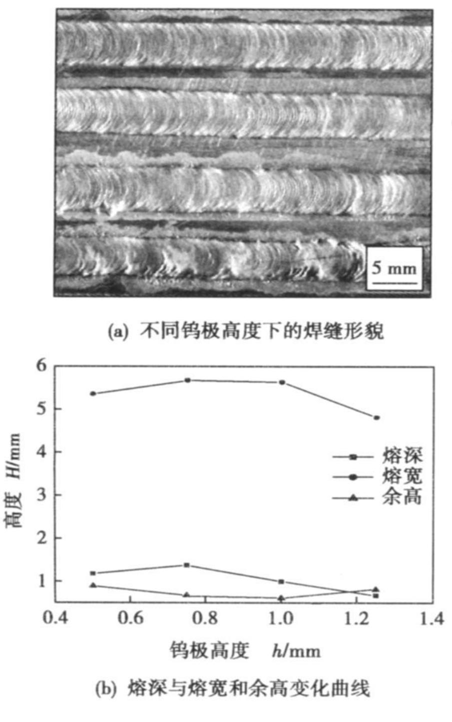

图 4　钨极高度对焊缝成形的影响

Fig. 4　Effect of electrode height on weld appearance

2.1.4　热源间距大小对焊缝成形的影响

图5 为其它参数相同(焊接电流为140 A, 焊接速度为800 mm/min, 钨极高度为0.75 mm, 送丝速度为2.5 m/min), 保持焊丝与钨极之间的距离不变, 改变热源间距 D_{LA} 大小时的焊缝成形情况。当 D_{LA} 为0.75~1.2 mm时, 激光与电弧的复合作用比较明显, 激光吸引电弧稳定作用于母材表面, 对母材的熔化效率高, 焊缝熔深较大。随着 D_{LA} 增大到1.2 mm左右, 焊丝、激光和电弧三者之间的距离逐渐匹配, 达到电弧能量主要熔化母材, 边缘电弧熔化焊丝的效果, 焊丝熔化充分, 同时激光的冲击作用明显, 焊接熔深达到最佳效果。当 D_{LA} 继续增大时, 电弧的稳定性下降, 使得电弧对焊丝的熔化效率下降, 不完全熔化的焊丝会伸到激光作用区域, 削弱了激光对母材的作用, 使熔深急剧下降。因此, 焊接过程中 D_{LA} 一般取1.2 mm左右。

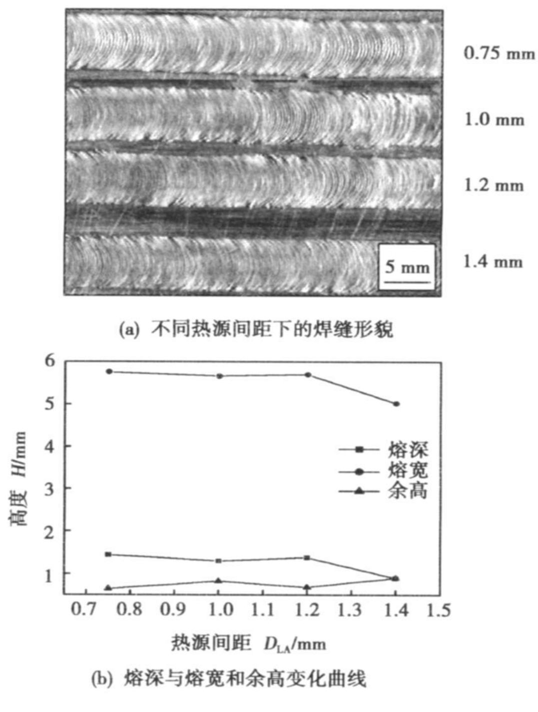

图 5　热源间距大小对焊缝成形的影响

Fig. 5　Effect of D_{LA} on weld appearance

送丝速度对焊缝成形也有影响, 在充分熔化的基础上, 合适的送丝速度可以保证焊丝熔化过程的连续性, 避免出现送丝过慢熔滴以大滴形式过渡或送丝过快出现焊丝偏离热源等缺陷, 提高焊缝成形质量。由此可知, 在复合热源冷填丝焊接过程中, 钨极高度和热源间距是影响焊缝成形的主要因素, 确定了钨极高度为0.75 mm、热源间距为1.2 mm左右的焊接参数范围; 而焊接电流、焊接速度等对焊缝成形的影响比较单一, 容易控制。

2.2 镁合金对焊试验

在堆焊试验的基础上,进行了2.5 mm厚镁合金板材的对焊试验。通过调节焊接参数,达到了电弧、激光束和焊丝三者之间的合理匹配,得到了复合热源冷填丝对焊最佳焊接参数,如表2所示。在该焊接参数下成功实现了镁合金板材的对接焊接,焊缝成形良好。

对镁合金激光—TIG复合热源冷填丝焊接和单TIG冷填丝焊接的焊缝成形和接头形貌进行对比分析,如图6所示,其中焊接电流为140 A,焊接速度为1 000 mm/min,送丝速度为2.5 m/min,钨极高度为0.75 mm,热源间距为1.2 mm。

表2 对焊焊接工艺参数

Table 2 butt welding parameters

焊接电流 I/A	焊接速度 v/(mm·min^{-1})	送丝速度 v_1/(m·min^{-1})	激光功率 P/W	钨极高度 H/mm	热源间距 D_{LA}/mm	氩气流量 Q/(L·min^{-1})
140	1 000	2.5	300	0.75	1.2	10

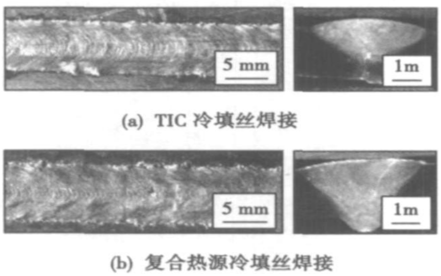

图6 焊缝成形对比

Fig. 6 Comparison of weld appearances

从图中可以看出,单TIG冷填丝焊接接头熔深和熔宽小,焊接余高较大,同时焊缝成形好,呈规则的波纹状;加入激光后,焊接接头熔深增大,达到前者的两倍,熔宽也比前者显著增大,相应地余高下降,焊缝表面成形趋于平整。这是因为激光吸引电弧向母材收缩,提高了电弧对母材的熔化效率,造成焊缝熔深和熔宽都增大。同时激光的加入可以提高电弧的稳定性。在高速焊接中,单TIG冷填丝焊接过程不稳定,容易造成飞溅等缺陷,导致焊接质量下降;而在复合热源冷填丝焊接过程中,电弧作用比较稳定,焊缝成形规则。但是在复合热源焊接过程中焊缝表面氧化很严重,需要加大氩气流量进行保护。

利用CSS—2205型电子万能试验机测试复合热源冷填丝焊接接头的拉伸性能(抗拉强度取3个试样的平均值)。结果表明,复合热源冷填丝焊接接头抗拉强度达到246.5 MPa,为母材(260 MPa)的95%,实现了优质的镁合金冷填丝焊接。

3 结 论

(1) 低功率激光氩弧复合热源冷填丝焊接中,钨极高度和热源间距是影响焊缝成形的主要因素,一般情况下钨极高度取0.75 mm,热源间距取1.2 mm左右。

(2) 成功实现了2.5 mm厚镁合金板材的对接焊接,焊缝成形美观,焊接过程稳定。

(3) 通过与单TIG冷填丝焊接比较,激光的加入使复合热源冷填丝焊接接头熔深达到前者的两倍,焊接速度达到1 200 mm/min,抗拉强度达到母材的95%左右,并且焊接过程稳定,实现了高速、优质的镁合金冷填丝焊接。

参考文献:

[1] Sun Z, Pan D, Wei J. Comparative evaluation of tungsten inert gas and laser welding of AZ31 magnesium alloy[J]. Science and Technology of Welding and Joining, 2002, 7(6): 343—351.

[2] Jefferson T B. Metals and how to weld them[M]. Cleveland, America: The James F. Lincoln Foundation, 1990.

[3] Wohlfahrt H, Rethlemeier M, Bouaifi B, *et al*. Metal-inert gas welding of magnesium alloys[J]. Welding and Cutting, 2003, 55(2): 80—84.

[4] 董长富, 刘黎明, 赵 旭. 变形镁合金填丝TIG焊接工艺及组织性能分析[J]. 焊接学报, 2005, 26(2): 33—36.

作者简介: 郝新锋, 男, 1983年出生, 博士研究生。主要从事镁合金激光—电弧复合热源焊接研究。发表论文1篇。

Email: liulm@dlut.edu.cn

similar materials

Cold-hot fatigue and wear-resistance of CoCrMoSi coatings
HUO Shubin[1], WANG Zhiping[2], WANG Jiajie[1], WANG Jixiao[1] (1. Harbin Welding Institute, Harbin 150080, China; 2. Civil Aviation University of China, Tianjin 300300, China). p73—76

Abstract: CoCrMoSi coating was deposited on CrZrCu with HVOF, and its cold-hot fatigue and war resistance were studied, analyzed and compared with NiCo plated coating widely applied in metallurgy industry. The results show that at 450 ℃ CoCrMoSi coating possesses high cold-hot fatigue property and it can endure 113 times cold-hot fatigue, while the plated coating only has 37.8 times. Both abrasive wear and adhesion abrasion occurred on the CoCrMoSi coating and NiCo plated coating. Adhesive wear is the main type of wear on the plated coating and it also has serious abrasive wear. But abrasive wear almost is not found on the CoCrMoSi coating, and it only has slight adhesive wear. The wear-resistance of the coating is much higher than that of the plated coating.

Key words: high velocity oxygen fuel; CoCrMoSi coating; cold-hot fatigue; wear-resistance property

Low powered laser-arc hybrid welding of magnesium alloy with cold filler wire
HAO Xinfeng, LIU Liming, LI Changmao (State Key Laboratory of Materials Modification, Dalian University of Technology, Dalian 116024, Liaoning, China). p77—80

Abstract: Low powered laser-arc hybrid welding of magnesium alloy with cold filler wire was studied. The effect of welding parameters on weld appearance and penetration was investigated in bead welding experiments of magnesium alloy plate with the thickness of 5 mm and the range of welding parameters was confirmed, such as the electrode height (about 0.75 mm) and the distance between laser and arc (about 1.2 mm). Based on this, magnesium alloy plate with the thickness of 2.5 mm was butt-welded successfully and the welding speed increases to 1 200 mm/min. The weld penetration of hybrid welding with cold filler wire is twice deeper that that of TIG welding and the tensile strength of hybrid welded joint achieves 95% of that of base metal, so magnesium alloy welded joint with high quality can be obtained by hybrid welding with cold wire at a high speed. Besides, the effect of laser pulses on welding process was analyzed.

Key words: magnesium alloy; low powered laser; hybrid thermal sources; welding with cold filler wire

Microstructure and transformation of electron beam welded joints of TiAl base alloy
CHEN Guoqing, ZHANG Binggang, HE Jingshan, FENG Jicai (State Key Laboratory of Advanced Welding Production Technology, Harbin Institute of Technology, Harbin 150001, China). p81—84

Abstract: The microstructural characteristics, phase composition and transformation of the electron beam welded (EBW) joints of Ti—43Al—9V—0.3Y alloy were investigated by means of the optical microscopy, X-ray diffraction, scanning electron microscopy, transmission electron microscopy and energy disperse spectrum. The results showed that the joint microstructure is mainly composed of $B2$ phase. The partial $\alpha_2+\gamma$ two-phase lamellar structure and granular γ_m phase are observed. The lanthanon Y exists as YAl_2 phase and refined grains. During the heat treatment and EBW of this alloy, different transformation of the liquid metal will take place duo to the different cooling rate in the cooling period. The lamellar microstructure and Widmanstaten structure will form because of low cooling rate. The faster cooling rate can lead to the formation of the γ_m phase. The ordering transformation only happens at very fast cooling rate. The different casting structures with different properties are obtained finally.

Key words: TiAl based alloy; electron beam welding; microstructure of joint; microstructure transformation

Effect of interactions among coating components on slag detachability of stainless steel electrode
YANG Tuoyu, MENG Gongge, YANG Deyun, CHEN Leida (School of Material Science & Engineering, Harbin University of Science and Technology, Harbin 150040, China). p85—88

Abstract: The experiments were designed according to the uniform design method and the data were processed with quadratic polynomial regression analysis. The 11 coating components seleced from the 16 components were taken as independent variables and the uniform design table $U_{30}(10^{11})$ was selected to design the experiment. The mathematical model was established and the interactions trend figures were obtained. The mathematical model indicates the complicated relations among the factors and the response. It also indicates the influences of each factor to the target by the coefficients. The trend figures of barium carbonate-titanium dioxide, barium carbonate-hematite and hematite-wollastonite can directly indicate the influences of interactions among coating components on the slag detachability. The titanium dioxide and hematite have positive effects at definite conditions. But the hematite doesn't have any influences on the slag detachability when wollastonite is at 5.0 wt%.

Key words: coating components; interaction; slag detachability; uniform design

Failure analysis on TIG welded joint between martensitic and austenitic stainless steels
LING Wei[1], GE Laohai[2], REN Zhen'an[3], SUN Daqian[3] (1. Changchun Institute of Optics, Fine Mechanics and Physics, Chinese Academy of Sciences, Changchun 130033, China; 2. Changchun Institute of Applied Chemistry, Chinese Academy of Sciences, Changchun 130022, China; 3. Key Laboratory of Automobile Materials, The Ministry of Education, Jilin University, Changchun 130025, China). p89—92

Abstract: Aiming at the leaking problem of the TIG welded joint between martensitic and austenitic stainless steels used in shipping facilities. Changes of microstructures and the microhardness distribution at different zones in the welded joint between 1Cr17Ni2 and 1Cr18Ni9Ti stainless steels were analyzed by optical microscope, scanning electronic microscope and microhardness tester. On the side of 1Cr17Ni2 base metal, ferrite became coarser in HAZ adjacent to the weld and its microhardness was relatively lower. At the zone in HAZ where the heated temperature was higher, martensite with high microhardness was obtained because of fast cooling. The